

The effect of structural defects on the compressive behavior of closed-cell Al foam

Insu Jeon ^{*}, Tadashi Asahina

Materials Research Institute for Sustainable Development, National Institute of Advanced Industrial Science and Technology (AIST), Shimoshidami, Moriyama-ku, Nagoya 463-8560, Japan

Received 12 January 2005; received in revised form 1 April 2005; accepted 2 April 2005
Available online 25 May 2005

Abstract

A simple experimental approach is attempted for this research. First, various size specimens of the closed-cell Al foam, ALPORAS® of Shinko Wire Co. Ltd., from $50 \times 50 \times 50 \text{ mm}^3$ to $8 \times 8 \times 8 \text{ mm}^3$ are fabricated using an electrical discharge machine for the uniaxial compression test. Second, structural defects such as partially coupled cells, missing cells and collapsed cells in fabricated specimens are carefully investigated by means of density measurement and surface observation. Then, the specimens are divided into two groups with or without structural defects and tested separately to compare the results. In this research, we present the effects of structural defects as well as specimen size on the compressive behavior of this Al foam.

© 2005 Acta Materialia Inc. Published by Elsevier Ltd. All rights reserved.

Keywords: Structural defects; Closed-cell Al foam; Experimental approach; Compressive behavior; Size effect

1. Introduction

Cellular material has lately attracted considerable attention as a lightweight component for transportation applications [1]. The compressive properties, such as the elastic modulus and plastic collapse stress of the cellular material, are important parameters for the mechanical design of the component under compression. Therefore, a number of research results have been published about the compressive characteristics of cellular material.

The tangential stiffness of the stress–strain curve under the loading process is smaller than that under the unloading process, giving us an insight into defining the elastic modulus of cellular materials, E_{UL} , measured during the unloading process [2,3]. The experimental analysis of deformation mechanisms in the closed-cell Al foam shows that the plateau stage in the compressive behavior is affected by the discrete bands of strain local-

ization that are formed and plastically collapsed in the material. The plastic collapse stress, σ_{pl} is governed by the first plastic collapse of the deformation bands [4,5]. Also, the effect of the specimen size, i.e., the ‘size effect’, on the reduction of the elastic modulus and plastic collapse stress of cellular materials has been reported [5–9]. The reduced constraint and increased area fraction of cell walls at the free surface, along with the decrease of the specimen size are regarded as the cause of the decrease of compressive properties. In these research efforts, however, the effect of defects included in the cellular materials on the specimen size has not been fully assessed.

Some numerical works elucidate the effect of processing-induced defects on mechanical properties of metallic foams. For example, using the numerical modeling of the idealized tetrakaidecahedral foam structure, it is found that Plateau borders have little effect on the elastic modulus and a moderate effect on the decrease of the plastic collapse stress. Meanwhile, cell face curvatures as well as corrugations have a significant effect on the

^{*} Corresponding author. Tel.: +81 52 736 7449, fax: +81 52 736 7400.
E-mail address: insu-jeon@aist.go.jp (I. Jeon).

decrease of the elastic modulus and plastic collapse stress [10,11]. Furthermore, the effects of wavy imperfections and cell shape variations on the decrease of the stiffness of cellular solids are confirmed using the wavy plate model and flat-faced non-uniform model [12,13].

Numerical studies using 2-D honeycomb models to account for the influence of geometric imperfections (i.e., fractured cell walls, missing cells, rigid inclusions, wrinkled cell walls, cell-size variations, etc.) on mechanical properties of the honeycomb structure have been carried out to provide guidelines for improving the properties of commercial metallic foams [14,15]. Among the imperfections, fractured cell walls show the largest diminishing effect on the yield strength. Missing cells have a large influence on both the elastic modulus and the yield strength. Moreover, rigid inclusions have a small stiffening effect on the elastic modulus and a negligible effect on the yield strength. Only a few experimental results, however, have been reported on the effect of processing-induced imperfections in cell walls, i.e., curvatures, corrugations and non-uniform microstructures, on the deformation behavior of Al cellular materials [16,17].

In this research, a simple experimental approach is attempted to analyze the effect of structural defects on the compressive behavior of the closed-cell Al foam. The structural defects, which are defined in this research as partially coupled cells, missing cells and collapsed cells, are generally formed during a manufacturing process and are easily found in actual closed-cell Al foams. Various size specimens from $50 \times 50 \times 50 \text{ mm}^3$ to $8 \times 8 \times 8 \text{ mm}^3$ are fabricated. Structural defects in the specimens are closely investigated by means of density measurements and surface observation. Then, two specimen groups with or without structural defects are separately tested for the purposes of comparison.

2. Experimental approach

2.1. Preparation of specimens

The closed-cell Al foam, ALPORAS[®] of Shinko Wire Co. Ltd. is selected as the specimen for the uniaxial compression test. For the fabrication of specimens, an electrical discharge machine (EDM) is utilized to ensure both surface flatness for the precise compression test and surface clearness for the investigation of structural defects in the specimens (see Fig. 1). A cube is selected for the geometric shape of specimens to prevent buckling during the compression process following the experimental results of the compressive behaviors of specimens with different heights [7]. The edge length of the specimen, $L = 50 \text{ mm}$, is selected to obtain very similar compressive behavior to that of a bulk foam material [6,7] and $L = 30, 20, 15, 10, 9, 8 \text{ mm}$ are selected in consideration of the volume fraction of structural defects. The average cell size is determined as $\bar{d} = 4.36 \text{ mm}$ in accordance with the definition of the equivalent diameter of a cell [3], which is measured from about 300 cells in the surface of fabricated specimens using the digital microscopic system, VHX-100 of Keyence Corp.

First, for the specimen group without structural defects, the density of the specimens is measured and the specimens within the range of the relative density $\bar{\rho} = \frac{\rho}{\rho_s} = 0.0815\text{--}0.0870$ are selected. Here, ρ is the density of the foam material and $\rho_s = 2.7 \text{ g/cm}^3$ is the density of the Al cell wall. This selection of specimens within a narrow range of relative densities helps in disregard specimens that include non-uniformly biased cell structures. Then, the surface of specimens is observed with the naked eye and digital microscopic system. Such observation can be a comparatively effective method to find specimens without structural defects in the small size specimens where $L = 15\text{--}8 \text{ mm}$. Because the average

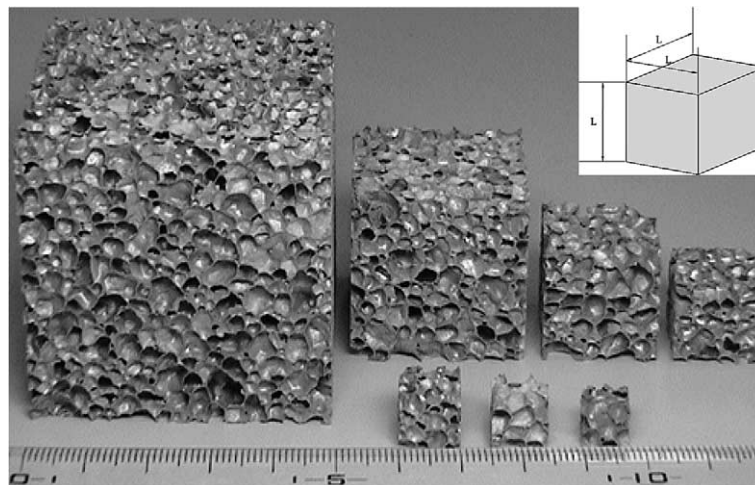


Fig. 1. The representative specimens without structural defects of each specimen size.

cell size \bar{d} is 4.36 mm, the average depth of about $\bar{d}/2$ from each surface of a specimen can be observed with the naked eye.

Then, the investigation of the inside of each cell on the surface with the digital microscopic system helps in estimating deeper cell structures and structural defects within the specimen. Particularly for the large specimens where $L = 50\text{--}20$ mm, it is extremely difficult to find the defects within the specimens because of the geometric complexity. However, these specimens with similar densities show similar compressive behavior to that of a bulk foam material, regardless of the defects within the specimens [5–7]. These results indicate that the volume fraction of structural defects in the large specimens of $L = 50\text{--}20$ mm decreases to that of bulk foam material. This should show a small reducing effect on the compressive behavior. Therefore, in this research these surface observations can be adopted to select specimens without structural defects for all sizes.

Because a large number of structural defects are inherently distributed in the closed-cell Al foam, the selection of specimens without defects needs lots of fabricated samples and elaborate efforts. Therefore, for the small specimens of $L = 15\text{--}8$ mm, over 200 samples for each size and for the large specimens of $L = 50\text{--}20$ mm, about 50 samples for each size were fabricated using EDM. The structural defects in the small specimens are observed with both the naked eye and digital microscopic system. The defects on the surface of the large specimens are observed only with the naked eye because of the small effect of the defects within the large specimens on the compressive behavior. At least seven specimens without structural defects were finally selected for each specimen size to guarantee the statistical reliability of the uniaxial compression test [8]. The representative specimens without structural defects of each specimen size are shown in Fig. 1.

For the specimen group with structural defects, the specimens were chosen from amongst the discarded samples after selecting the specimens without structural defects. Through the density measurement, specimens with defects within the range of the relative density $\bar{\rho} = 0.0822\text{--}0.0867$ were finally selected. Each structural defect included in each specimen size is shown in Fig. 2. The partially coupled cell has the residual cell wall between two cells, the missing cell shows a deep hole within a cell and deformable inclusions are shown around the collapsed cell. These structural defects can be regarded as actual defects equivalent to modeled ones such as the fractured cell wall, the missing cell and the rigid inclusion in the 2-D honeycomb structure presented by Chen et al. [14,15].

2.2. Uniaxial compression tests

The universal testing machine, AG-I of Shimadzu Corp. was used for the uniaxial compression test and the designed software for AG-I, TRAPEZIUM was used to record displacement and loading results. The specimens of $L = 50, 30$ mm were compressed by 100 kN load cell between a steel spherical compression platen and circular compression platen. The specimens of $L = 20\text{--}8$ mm were compressed by 5 kN load cell between two steel circular compression platens. The diameter of each platen, $D = 100$ mm, was sufficiently larger than the size of each specimen. The parallelism between the two platens was carefully adjusted through examination of the contact surface between them before the compression test. The displacement rate 1 mm/min was applied on the top surface of each specimen as an external loading (see Fig. 3). All specimens were loaded up to 80% of the strain to obtain the whole compressive behavior. Because unloading curves are essentially invariant with the strain at the small strain state [2],

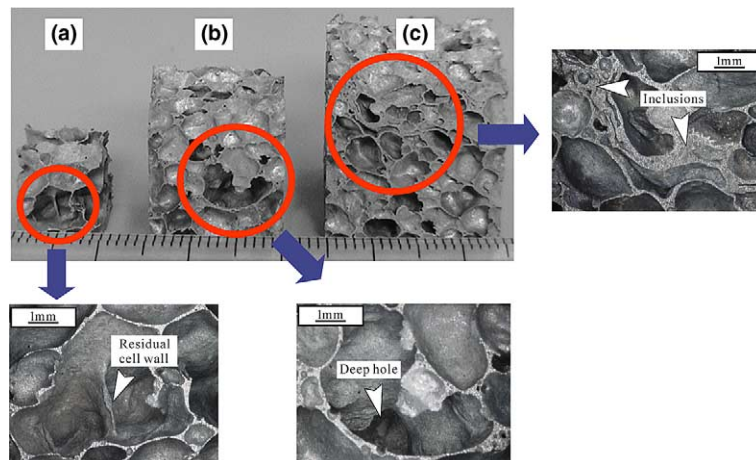


Fig. 2. (a) The partially coupled cell, (b) missing cell and (c) collapsed cell in each specimen size.

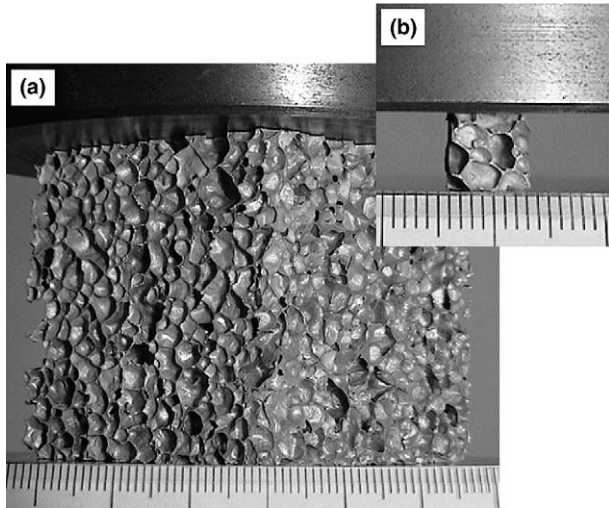


Fig. 3. Two representative specimens of (a) $L = 50$ mm under a 100 kN load cell and (b) $L = 8$ mm under a 5 kN load cell.

the unloading process for measuring the elastic modulus was begun at 6% of the strain for each specimen soon after the plastic collapse stress. Then the reloading process was continued up to the final strain.

For measuring the elastic modulus of each specimen, two characteristics of the universal testing machine, AG-I, were considered. One is the machine compliance. During the uniaxial compression test, a strain gauge or an extensometer is necessary for the precise measurement of the specimen strain. However, because of the structural weakness and the surface condition of cellular materials, it is extremely difficult to measure the strain with those strain-sensing systems. In fact, the displacement recorded by the software, TRAPEZIUM, during the compression test is taken as the sum of displacements in the specimen and the testing machine. For obtaining the specimen displacement, the displacement of the testing machine has to be subtracted from the recorded one by the software. Therefore, the machine compliance, which shows the relation between the displacement of the testing machine and the applied loading, has to be considered for precise specimen displacement [18]. Fig. 4 shows two measured machine compliances of the testing machine, AG-I with a 5 kN and a 100 kN load cell for obtaining the displacement of each specimen. The specimen strain will be the measured specimen displacement divided by the edge length of the specimen, L .

The other characteristic of the AG-I is the accuracy of the compression loading measured by the testing machine. The measured loading less than (load cell capacity)/100, which is the lower bound of the compression accuracy of the testing machine AG-I includes the machine operation errors. Therefore, for measuring the elastic modulus, the linear interval between the maximum stress and the stress corresponding to the lower

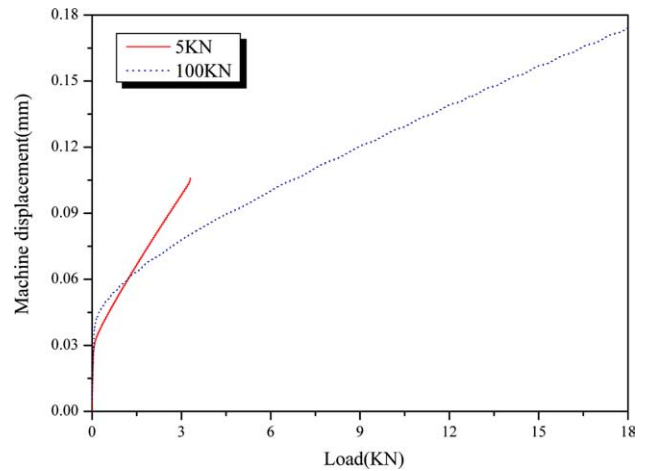


Fig. 4. Machine compliances of a (a) 5 kN and (b) 100 kN load cell.

bound of the compression accuracy in the stress–strain curve of the unloading process has to be considered. In this research, we select the linear 0.35 MPa interval between 1.25 and 0.9 MPa for the specimens of $L = 8$, 9 mm and the linear 0.5 MPa interval between 1.2 and 0.7 MPa for the specimens of $L = 50$ –10 mm.

3. Results and discussion

The measured compressive stress–strain curves for the specimen group without structural defects are shown in Fig. 5. Of all test results, seven curves for each specimen size are presented in Fig. 5(a)–(g). The consistent stress–strain behavior with small variations along with each specimen size is obtained, although the small specimens of $L = 15$ –8 mm are used for the uniaxial compression test. However, Fig. 5(f) and (g) for the specimens of $L = 9$, 8 mm show some stress deviations in the stress–strain curves in the strain range 0.2–0.6, compared with the curves for the large specimens of $L = 50$ –20 mm. Because of the difficulty in finding perfect small specimens without any structural defects, some selected specimens, in fact, include parts of the defects. These affect the compressive behavior and are believed to cause the deviations. Slightly different stress–strain behavior soon after the plastic collapse stress is found between the large specimens of $L = 50$ –20 mm and the small specimens of $L = 15$ –8 mm. Because the first plastic collapse band affects the stress–strain behavior at this stage [5], it is thought that this difference stems from a small number of cell structures in the small specimens that produce a small scale first band collapse and a small resistance to the compression loading after the plastic collapse.

From these curves, the compressive properties of each specimen without structural defects are measured. The obtained average density, elastic modulus and

plastic collapse stress with their standard deviations are given in Table 1. The standard deviations are small. Furthermore, Table 1 shows that the measured elastic modulus and plastic collapse stress stay within the range of previously published ones [5–8].

In Fig. 6, the measured elastic modulus, E_{UL}^* and plastic collapse stress, σ_{pl}^* for each specimen size normalized by those of a bulk cellular material, i.e., $E_{UL,Bulk}^*$ and $\sigma_{pl,Bulk}^*$, are plotted against the characteristic length of test specimens divided by the average cell size, L^*/\bar{d} . The results of Bastawros et al. [5] and Andrews et al. [6] that show the well-known ‘size effect’ of cellular materials are plotted together for comparison. The characteristic length L^* of this research and Andrews et al. [6] are the edge length, L and the width of the test specimen, respectively. The values E_{UL}^* and σ_{pl}^* of this research and Andrews et al. [6] are averaged ones for each specimen size and $E_{UL,Bulk}^*$ and $\sigma_{pl,Bulk}^*$ are chosen from E_{UL}^* and σ_{pl}^* of the specimen of $L^* = 50$ mm, respectively. The standard errors for the average results in this research are calculated and indicated with error bars to

show the accuracy of each data point. In particular, the characteristic length L^* of Bastawros et al. [5] means the thickness of the test specimen. The values E_{UL}^* and σ_{pl}^* are approximately obtained from their Figs. 3 and 4(b), and $E_{UL,Bulk}^*$ and $\sigma_{pl,Bulk}^*$ are selected from their fitted curves at $L^*/\bar{d} = 9$.

Two interesting results are found in Fig. 6(a) and (b). One is the remarkably improved values of $E_{UL}^*/E_{UL,Bulk}^*$ for the specimens of $L^*/\bar{d} < 6$ without structural defects compared with the ones of Andrews et al. [6]. The other is the size independent values of $\sigma_{pl}^*/\sigma_{pl,Bulk}^*$ for the specimens of $L^*/\bar{d} \geq 1.834$ without defects. Note that the normalized values, $E_{UL}^*/E_{UL,Bulk}^*$ and $\sigma_{pl}^*/\sigma_{pl,Bulk}^*$ in this research show the considerably reduced scattering effect compared with the results of Bastawros et al. [5]. Moreover, these two values around $L^*/\bar{d} \sim 2$ are shown to be similar to the $E_{UL}^*/E_{UL,Bulk}^*$ and approximately 10–15% improved on the $\sigma_{pl}^*/\sigma_{pl,Bulk}^*$ of Bastawros et al. [5].

The differences of each compression test are the use of different geometric shapes and fabrication methods for the test specimen. However, in this research the

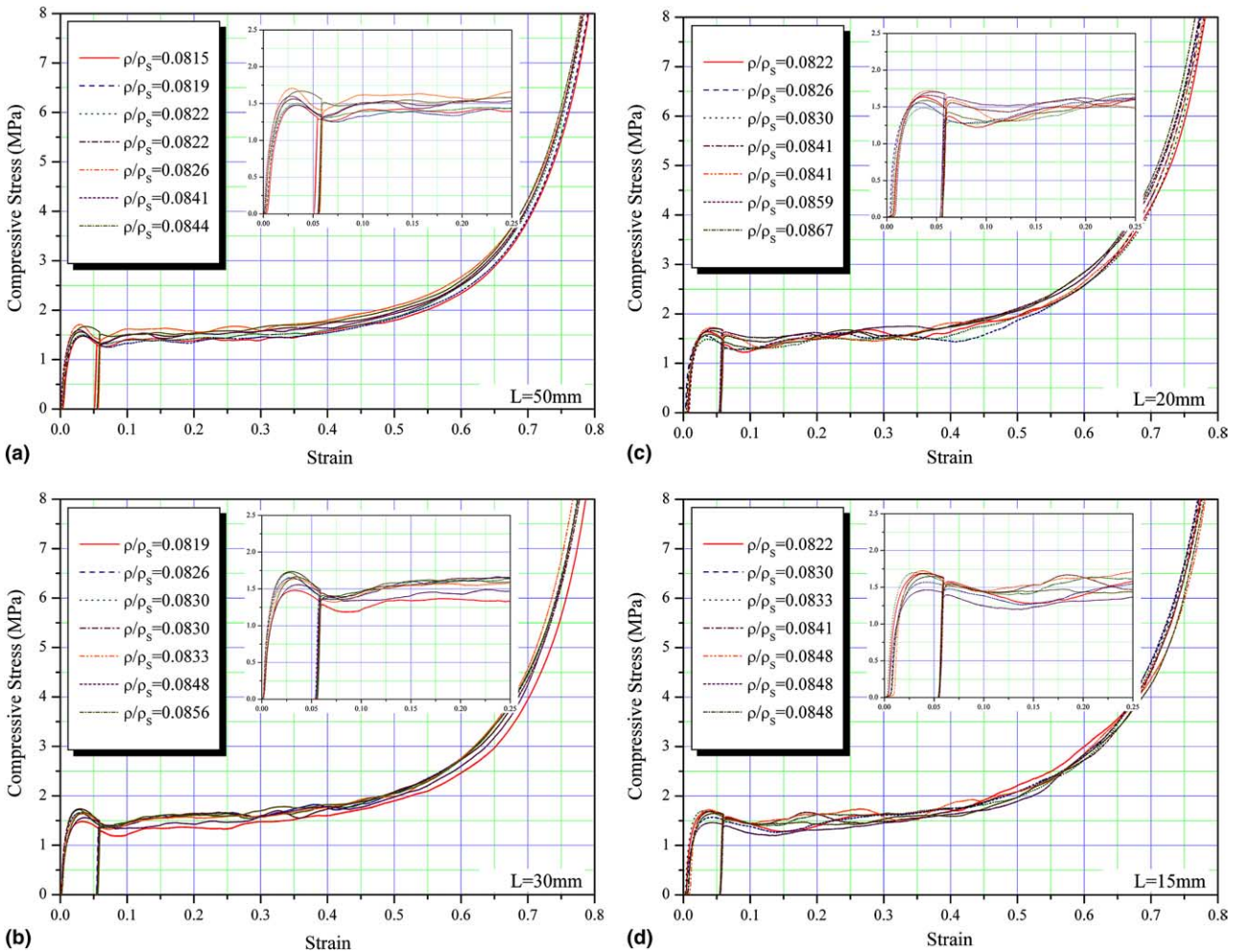


Fig. 5. The compressive stress–strain curves for the specimens of (a) $L = 50$ mm, (b) $L = 30$ mm, (c) $L = 20$ mm, (d) $L = 15$ mm, (e) $L = 10$ mm, (f) $L = 9$ mm and (g) $L = 8$ mm without structural defects. Insets are expanded graphs of the initial deformation stage.

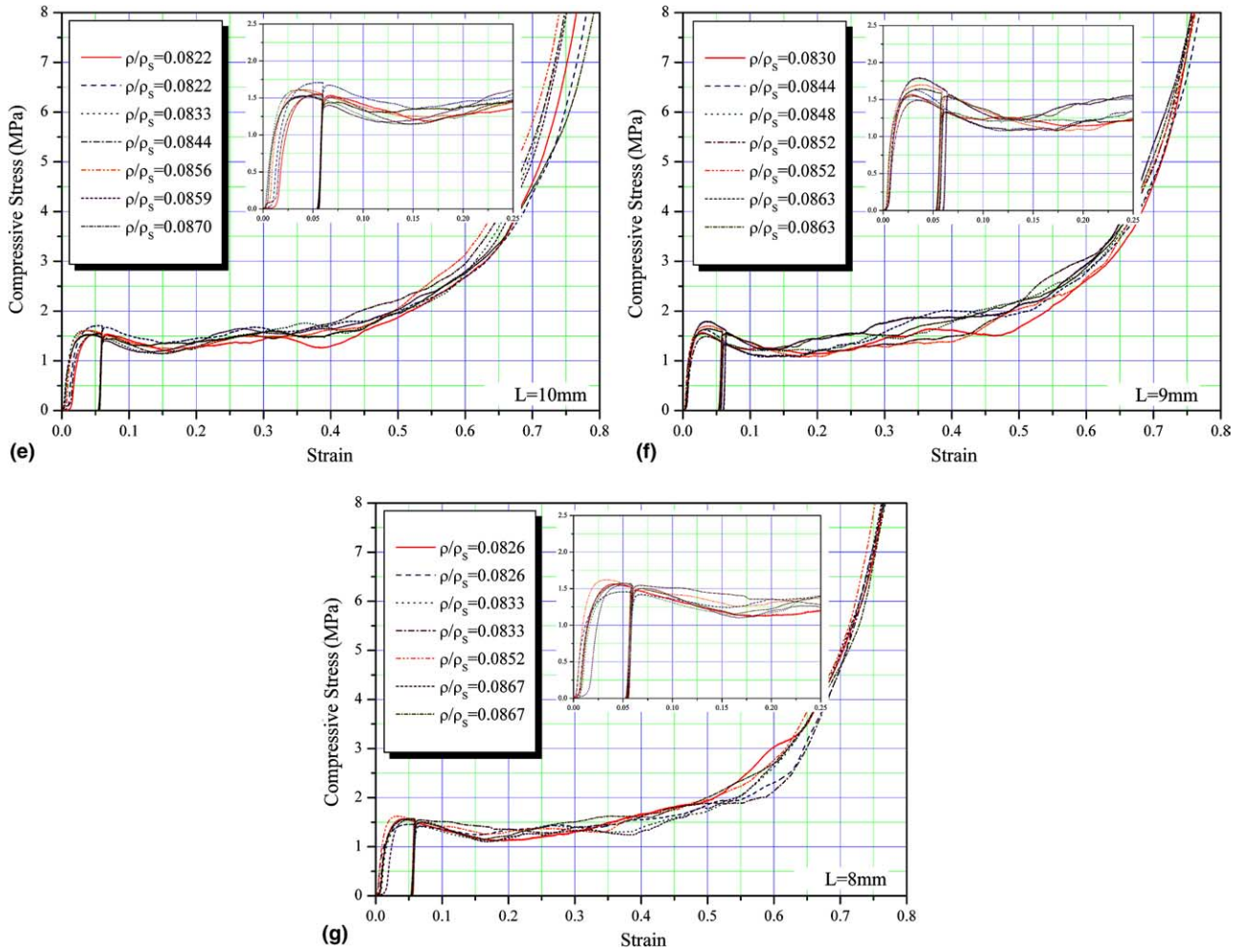


Fig. 5 (continued)

Table 1
The compressive properties of specimens without structural defects

L (mm)	Density (g/cm ³)		E _{UL} (MPa)		σ _{pl} (MPa)	
	Average	Standard deviation	Average	Standard deviation	Average	Standard deviation
50	0.224	0.00287	777.631	57.615	1.550	0.0651
30	0.225	0.00334	762.736	69.185	1.615	0.0102
20	0.228	0.00416	737.820	35.163	1.612	0.0736
15	0.227	0.00271	726.774	91.907	1.650	0.0825
10	0.228	0.00470	663.435	69.107	1.588	0.0600
9	0.230	0.00323	627.662	74.811	1.605	0.0794
8	0.230	0.00527	584.881	89.304	1.568	0.0718

differences should mainly be in the investigation of structural defects. Therefore, a large part of the serious decrease of the values, $E_{UL}^*/E_{UL,Bulk}^*$ and $\sigma_{pl}^*/\sigma_{pl,Bulk}^*$, particularly in the small size specimens which are known as the ‘size effect’ of the closed-cell Al foam is attributed to the effect of structural defects from these comparisons. These reducing effects on the measured elastic modulus and plastic collapse stress in the small size specimens will clearly appear in Fig. 8(a).

Fig. 7 shows the representative stress–strain curves of each specimen size without structural defects. Of the seven stress–strain curves in each of Fig. 5(a)–(g), the curve that has the closest plastic collapse stress to the average one is selected and plotted in Fig. 7. Even though the small size specimen shows the reduced elastic modulus E_{UL}^* of the closed-cell Al foam (see Fig. 6(a)), that effect on the whole deformation behavior under compression is small. Therefore, with the size independency of the

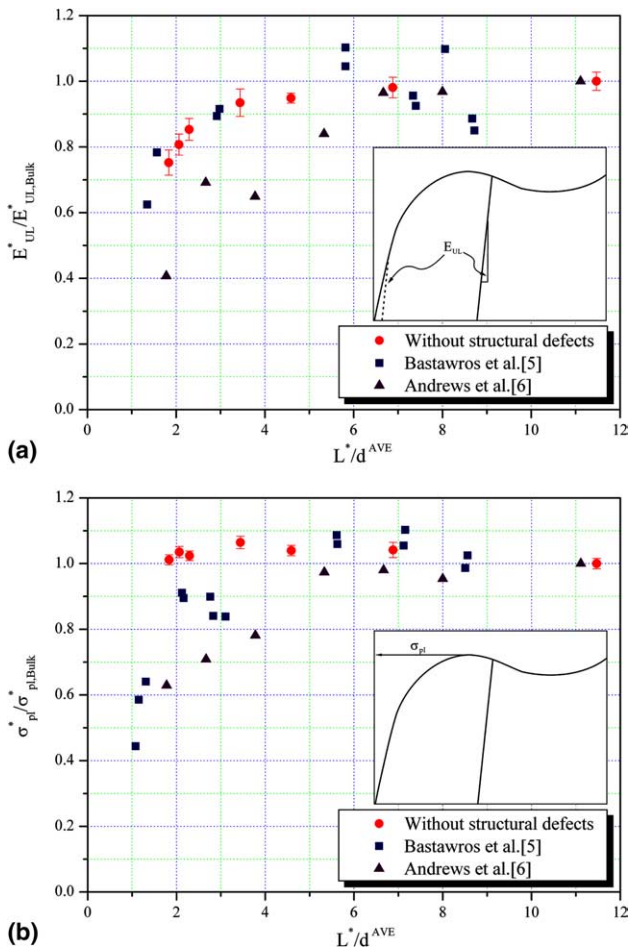


Fig. 6. (a) The measured elastic modulus and (b) plastic collapse stress for each specimen size normalized by those of a bulk cellular material plotted against the characteristic length of test specimens divided by the average cell size.

plastic collapse stress in Fig. 6(b), good agreement is found in the stress–strain curves of each specimen size.

However, for the specimen of $L = 8$ mm, a somewhat reduced stress level after the plastic collapse stress is found. In particular, the agreement on the stress–strain curves in Fig. 7 indicates that it may be feasible for the numerical analysis to investigate the deformation and failure mechanisms of the bulk cellular material, using the direct modeling of small actual specimens without structural defects. This is because the small specimens of $L = 10, 9$ mm show nearly similar stress–strain responses to that of the bulk cellular material. Recently published results of Youssef et al. [19] increase the possibility of the finite element analysis using the small actual closed-cell Al foam. They introduce a methodology for the numerical analysis of a polyurethane foam cube with a edge length of 0.5 mm using X-ray microtomography, the software for mesh generation on the geometric surface models that are converted from the tomographic data and the package code for the finite element method.

Fig. 8(a) shows the effect of partially coupled cells and missing cells on the stress–strain response of the closed-cell Al foam. Because of their morphological similarity and the difficulty distinguishing between them in the actual cellular material, we deal with the effects of these defects collectively and plot the measured results together. Considering the volume fraction of these defects, the specimens of $L = 15, 10$ mm that have densities close to the average one are selected. Seriously deviated stress–strain curves from those of specimens without structural defects are obtained because of the geometric irregularity of these defects. Using these curves, the compressive properties are measured and listed in Table 2.

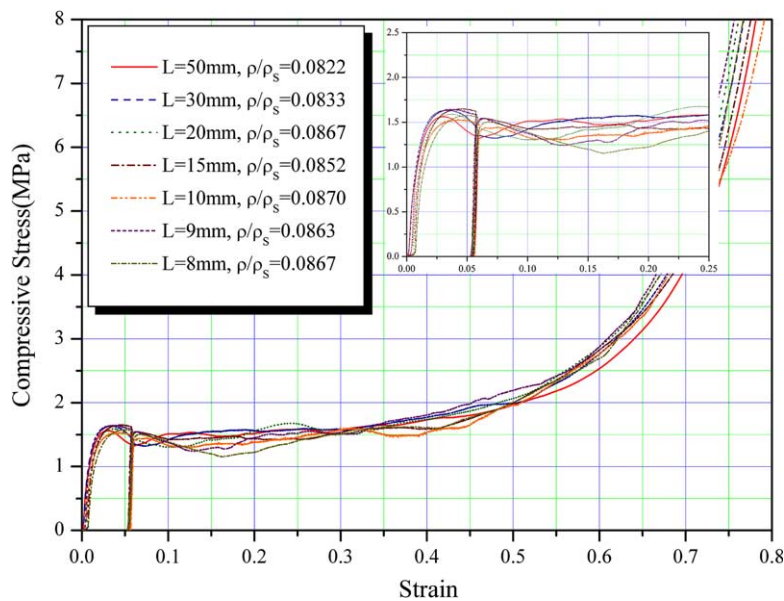


Fig. 7. The representative stress–strain curves of various size specimens without structural defects. Inset is an expanded graph of the initial deformation stage.

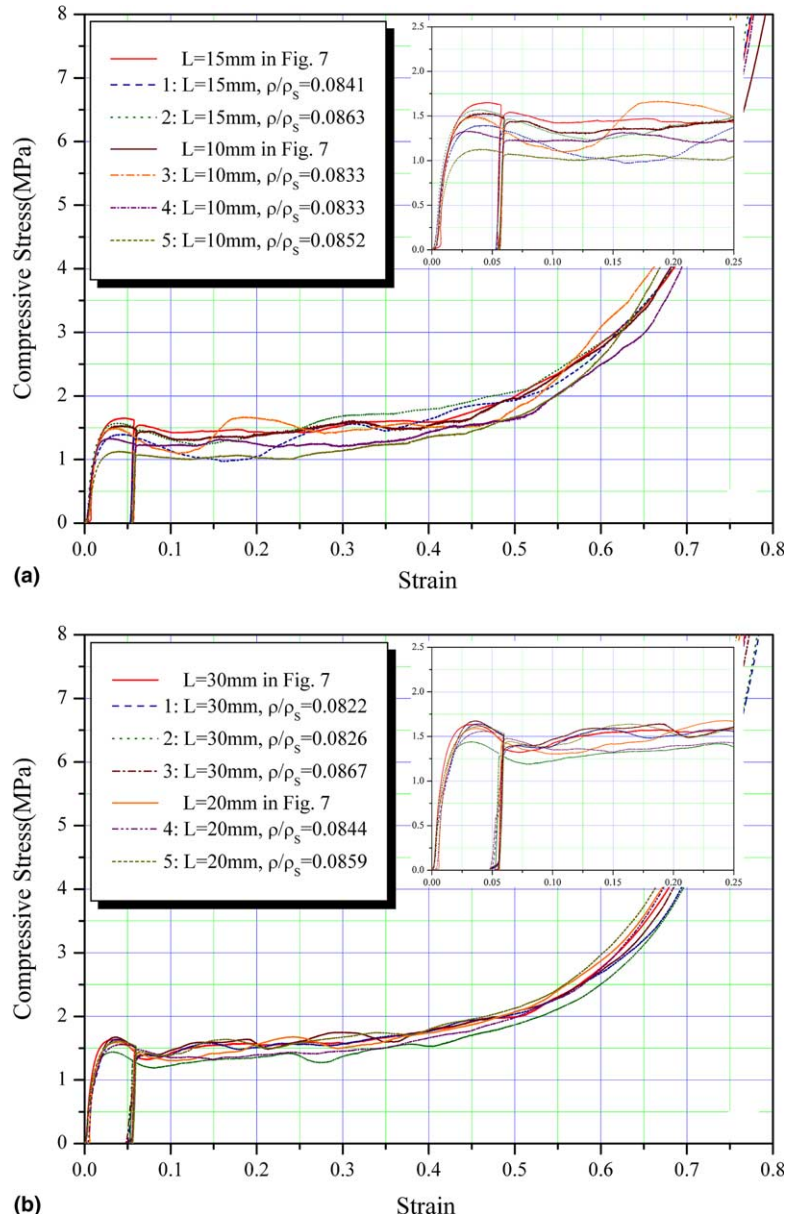


Fig. 8. The compressive stress–strain curves for specimens with (a) partially coupled cells and missing cells and (b) collapsed cells. Insets are expanded graphs of the initial deformation stage.

The results in Table 2 show that partially coupled cells and missing cells significantly reduce the elastic modulus and plastic collapse stress of the closed-cell Al foam. However, it is also found that only a few specimens with the defects produce a similar plastic collapse stress to the average one. This result suggests that the effect of these defects on the plastic collapse stress should be small when the deformation induced from the defects does not contribute to the first plastic collapse of the deformation band. The effects of partially coupled cells and missing cells on the compressive properties show a good agreement with the effects of fractured cell walls and missing cells calculated by Chen et al. [14,15].

Table 2

The compressive properties of specimens including partially coupled cells and missing cells

<i>L</i> (mm)		Graph no.	E_{UL} (MPa)	σ_{pl} (MPa)
Ave. E_{UL} (MPa)	Ave. σ_{pl} (Mpa)			
<i>L</i> = 15		1	659.484	1.397
	726.774	2	663.142	1.572
<i>L</i> = 10		3	590.506	1.494
		4	587.595	1.334
	663.435	5	509.954	1.131

Fig. 8(b) shows the effect of collapsed cells on the compressive behavior of closed-cell Al foam. The measured elastic modulus and plastic collapse stress are

Table 3
The compressive properties of specimens including collapsed cells

L (mm)		Graph no.	E_{UL} (MPa)	σ_{pl} (MPa)
Ave. E_{UL} (MPa)	Ave. σ_{pl} (Mpa)			
$L = 30$		1	517.427	1.644
		2	624.173	1.443
	762. 736	3	555.770	1.678
$L = 20$		4	624.293	1.560
	737.820	5	589.441	1.612

listed in Table 3. Because the size of a collapsed cell is larger than that of a partially coupled cell or a missing cell, the specimens of $L = 30, 20$ mm with the collapsed cell are selected. From the results in Table 3, it is found that the collapsed cell has a notable decreasing effect on the elastic modulus and a small effect on the plastic collapse stress. These results are regarded as showing that the collapsed cell contributes to the increase of the elastic deformation in the cellular material rather than the first plastic collapse of the deformation bands. The effect of the collapsed cell on the plastic collapse stress of the closed-cell Al foam shows a similar trend to the negligible effect of rigid inclusions on the yield strength of the 2-D honeycomb presented by Chen et al. [15]. However, the collapsed cell effect on the elastic modulus shows a somewhat opposite trend to the small stiffening effect of rigid inclusions on the elastic modulus of the 2-D honeycomb.

4. Conclusions and further study

By means of experimental investigation, the effect of structural defects on the compressive behavior of the closed-cell Al foam named ALPORAS[®] is analyzed. Among the structural defects, the partially coupled cell and missing cell cause serious deviations in the stress–strain response and significantly reduce the elastic modulus and plastic collapse stress of the closed-cell Al foam. The collapsed cell has a notable reducing effect on the elastic modulus and a small effect on the plastic collapse stress. Also, these structural defects contribute to the serious decrease of the values, $E_{UL}^*/E_{UL,Bulk}^*$ and $\sigma_{pl}^*/\sigma_{pl,Bulk}^*$, particularly in the small size specimens, which is known as the ‘size effect’ of the closed-cell Al foam. Therefore, the reduction of structural defects

through the improvement of the manufacturing technique is essential to improve the compressive properties of cellular materials.

In particular, the agreement of the stress–strain curves of each specimen size without structural defects obtained in this research makes it feasible for the numerical analysis to be used to investigate the deformation and failure mechanisms of the bulk cellular material. Therefore, numerical analysis using the direct modeling of the small actual closed-cell Al foam without structural defects is now subject to further study.

Acknowledgments

I. Jeon thanks Dr. Yasuo Yamada and Dr. Akira Watazu of AIST for precious discussions about the experimental process, and Mr. Kiyotaka Katou and Mr. Takahiko Yamada of AIST for technical support. Dr. Hyon-Jeong Lee is also acknowledged for valuable and helpful advice.

References

- [1] Banhart J. Prog Mater Sci 2001;46:559.
- [2] Sugimura Y, Meyer J, He MY, Bart-Smith H, Grenstedt J, Evans AG. Acta Mater 1997;45:5245.
- [3] Simon AE, Gibson LJ. Acta Mater 1998;46:3109.
- [4] Evans AG, Hutchinson JW, Ashby MF. Prog Mater Sci 1999;43:171.
- [5] Bastawros AF, Bart-Smith H, Evans AG. J Mech Phys Solids 2000;48:301.
- [6] Andrews EW, Gioux G, Onck P, Gibson LJ. Int J Mech Sci 2001;43:701.
- [7] Chino Y, Mabuchi M, Yamada Y, Hagiwara S, Iwasaki H. Mater Trans 2003;44:633.
- [8] Ramamurty U, Paul A. Acta Mater 2004;23:869.
- [9] Rakow JF, Waas AM. Mech Mater 2005;37:69.
- [10] Simon AE, Gibson LJ. Acta Mater 1998;46:2139.
- [11] Simon AE, Gibson LJ. Acta Mater 1998;46:3929.
- [12] Grenstedt JL. J Mech Phys Solids 1998;46:29.
- [13] Grenstedt JL, Tanaka K. Scripta Mater 1999;40:71.
- [14] Chen C, Lu TJ, Fleck NA. J Mech Phys Solids 1999;47:2235.
- [15] Chen C, Lu TJ, Fleck NA. Int J Mech Sci 2001;43:487.
- [16] Andrews E, Sanders W, Gibson LJ. Mater Sci Eng A 1997;270:113.
- [17] Markaki AE, Clyne TW. Acta Mater 2001;49:1677.
- [18] Kalidindi SR, Abusafieh A, El-Danaf E. Exp Mech 1997;37:210.
- [19] Youssef S, Maire E, Gaertner R. Acta Mater 2005;53:719.